Desalination and Water Treatment
www.deswater.com
doi: 10.5004/dwt.2019.24972

172 (2019) 115–124
December

Green synthesis of Pd/Fe_3O_4 bimetallic nanoparticles: catalytic in-situ generations of H_2O_2 for heterogeneous Fenton-like decolorization of Basic Red 46 and Direct Red 23

M. Ergüt*, A. Özer

Faculty of Engineering, Department of Chemical Engineering, Mersin University, Çiftllikköy Campus F-Block, Yenişehir, Turkey, email: memduha.ergut@gmail.com (M. Ergüt)

Received 19 May 2019; Accepted 26 September 2019

ABSTRACT

In this study, Pd/Fe_3O_4 bimetallic nanoparticles (Pd/Fe_3O_4 NPs) were biosynthesized by aqueous lemon (*Citrus limon (L.) Burm. f.*) leaves extract as a reducing agent and were characterized by scanning electron microscopy, dynamic light scattering (DLS), and X-ray diffraction analysis methods. The characterization studies confirmed the synthesis of Pd/Fe_3O_4 NPs successfully. According to DLS analysis, the mean hydrodynamic radius of Pd/Fe_3O_4 NPs was found to be 64.95 nm. In the second part of the study, Pd/Fe_3O_4 NPs were utilized as a common heterogeneous catalyst for both in-situ H_2O_2 synthesis by formic acid decomposition in the presence of oxygen and heterogeneous Fenton-like decolorization of Basic Red 46 (BR 46) and Direct Red 23 (DR 23) azo dyes. To determine the decolorization efficiency of heterogeneous Fenton-like reaction which was carried out by in-situ H_2O_2 synthesis, the effects of reaction parameters such as the concentration of formic acid, initial pH of dye solutions, initial dye concentrations and catalyst concentration were investigated for both dye decolorization processes. Consequently, Pd/Fe_3O_4 NPs displayed high decolorization performances for BR 46 and DR 23 in the range of 25–200 mg/L BR 46 concentration and in the range of 25–75 mg/L DR 23 concentration.

Keywords: Palladium-iron oxide bimetallic nanoparticles; *Citrus limon*; in-situ H_2O_2; Heterogeneous Fenton-like reaction; Catalyst; Basic Red 46; Direct Red 23

1. Introduction

In recent years; the wastewater treatment methods are called as advanced oxidation processes (AOPs), including homogeneous Fenton reaction ($Fe(II)/H_2O_2$), photo-Fenton reaction ($Fe(II)/H_2O_2/UV$), ozonation (O_3), wet peroxide ozonation (O_3/H_2O_2), H_2O_2/UV, heterogeneous Fenton-like processes and photocatalytic (TiO_2/UV and ZnO/UV) processes have attracted considerable attention for the removal of toxic and carcinogenic organic/inorganic pollutants from water sources. Heterogeneous Fenton-like reaction is one of the popular AOPs. Hydrogen peroxide (H_2O_2) is the most preferred oxidizing agent because of its environmental friendliness, the rapid and easy formation of hydroxyl radicals for degradation of contaminants in heterogeneous Fenton-like reactions. However, the problems such as, the use of hydrogen peroxide is much higher than which is converted into hydroxyl radicals during the reaction due to the hydrogen peroxide is fed to the system in bulk, the cost of commercial hydrogen peroxide is expensive, difficulties in synthesis method, danger of transport and storage, affect the process negatively. Therefore, the indirect synthesis of H_2O_2 catalytically in the reaction medium without adding H_2O_2 from the outside (in-situ hydrogen peroxide synthesis) offers an advantage in avoiding problems caused by unnecessary

* Corresponding author.

Presented at the 4th International Conference on Recycling and Reuse 2018 (R&R2018), 24–26 October 2018, Istanbul, Turkey

use of H_2O_2 in the heterogeneous Fenton-like reactions. In this method which is called as in-situ H_2O_2 synthesis; the catalytic decomposition of the organic compounds such as formic acid, hydrazine hydrate, and hydroxylamine, etc., which have substituted hydrogen in their structure and mostly used for hydrogen production, leads to hydrogen gas generation and H_2O_2 can be synthesized by the reaction of hydrogen and oxygen added in reaction media [1,2]. Therefore, the in-situ generation of H_2O_2 by metal nanoparticle catalyzed heterogeneous Fenton-like reaction appears to be a cost-effective option because of the use of a single catalyst in the H_2O_2 synthesis and degradation process. So, in-situ generation of H_2O_2 can not only improve the storage and transportation safety of H_2O_2 but also decrease the capital and operation costs [3].

There are many studies in the literature investigating the direct H_2O_2 synthesis from H_2 and O_2 by using Pd and Pd supported metal catalysts [4–6]. Furthermore, many studies were carried out for the generation of H_2 as a result of catalytic decomposition of formic acid by Pd containing supported metal catalysts such as PdAu@Au/C core–shell catalyst, graphene/PtAu alloy nanoparticles, nano-NiAuPd alloy, AuPd/TiO_2 nanofibers, AgAuPdNPs/graphene, Ag-Pd core–shell nanocatalyst, phenylamine modified SBA-15 supported PdAgNPs [7–13]. Also, there are a limited number of studies about the generation of H_2O_2 by the catalytic decomposition of organic compounds such as formic acid, hydrazine hydrate, and hydroxylamine. Generally, again Pd nanoparticles containing catalysts as Pd/γ-Al_2O_3 and Pd/Al_2O_3 have been used in these reported studies [14,15].

Therefore, in-situ H_2O_2 synthesis during the AOPs from the organic compounds containing substituted hydrogen such as formic acid, hydrazine hydrate, and hydroxylamine is a new attempt that attracted attention recently. In the literature, only a few studies have been reported in which organic pollutant degradation is studied by in-situ H_2O_2 synthesis from organic compounds containing substituted hydrogen [16,17]. In these studies, generally Pd and Fe containing bimetallic and supported composite nanoparticles as semi-heterogeneous (Pd/Al_2O_3 + soluble Fe^{2+}), fully heterogeneous (FePd/Al_2O_3) and Pd/PdO/Fe_2O_3 nanoparticles in SBA-15 were used as catalysts. The relatively small number of studies in this field requires the improvement of this method and the development of cost-effective heterogeneous catalysts.

The effective degradation of many types of organic pollutants was carried out by nanomaterial-catalyzed Fenton-like processes. Examples of nanoparticles used in the literature include zero-valent iron nanoparticles, iron-containing bimetallic nanoparticles (Fe/Pd-NPs, Fe/Ni-NPs, Fe/Cu-NPs), nano α-Fe_2O_3, CuO nanoparticles, ferrospinel nanoparticles ($ZnFe_2O_4$, $MgFe_2O_4$, $NiFe_2O_4$) [1].

The use of plant leaves extracts as a reducing agent is a promising approach for preparing metal/metal oxide nanoparticles due to this approach offers many advantages such as being simple and efficient, low-cost, environmentally friendly, readily available [18]. The lemon, (*Citrus limon (L.) Burm. f.*) is a species of a small evergreen tree in the flowering plant family Rutaceae, native to Asia [19]. In this regard, lemon leaves could be entirely appropriate candidates for green synthesis of metallic nanoparticles for the removal of toxic pollutants from water supplies.

In this study, Pd/Fe_3O_4 bimetallic nanoparticles were green synthesized as a catalyst by aqueous lemon leaves extract as a reducing agent for both in-situ H_2O_2 synthesis and the decolorization of Basic Red 46 (BR 46) and Direct Red 23 (DR 23) azo dyes with heterogeneous Fenton-like reactions for the first time.

BR 46 and DR 23 dyes were selected as model dye pollutants in this study. DR 23 which is an anionic direct azo dye is widely used in several industries such as textiles, paper, and cosmetics. As DR 23 has a diazo group, it is not rapidly biodegraded and it has toxicity and carcinogenic nature. BR 46 is a cationic synthetic azo dye which is extensively used in the textile industry. It has a mono azo group and it is also mutagenic and carcinogenic due to its biodegradability is difficult [20,21].

In this study, it was aimed that the Pd centers of synthesized catalyst will work for HCOOH decomposition to produce H_2O_2 with feeding O_2 to reaction media, and Fe centers were responsible for the decomposition of H_2O_2 into hydroxyl radicals for Fenton-like decolorization of studied model dyes. The optimum reaction conditions of heterogeneous Fenton-like reaction which was carried out by in-situ H_2O_2 synthesis were investigated for both dye decolorization processes.

2. Materials and methods

2.1. Materials

Lemon leaves were collected from lemon trees grown in Tece/Mersin, Turkey. All the chemicals used in experiments were of analytical grade and were used without further purification. BR 46 dyestuff was supplied by Dye Star with commercial name is Astrazon Red FBL. BR 46 was of commercial purity (Type: Cationic, Mw: 322 g/mol, λ_{max}: 530 nm). The chemical structure of BR 46 is shown in Fig. 1a, DR 23 which is a water-soluble anionic direct azo dye, was purchased from Sigma-Aldrich (USA). DR 23 was of commercial purity (Type: Anionic, Mw: 813.73 g/mol, λ_{max}: 507 nm). The chemical structure of DR 23 is presented in Fig. 1b. $FeSO_4{\cdot}7H_2O$ and Na_2CO_3 were supplied from Carlo Erba (Barcelona), and $PdCl_2$ was provided from Sigma-Aldrich (USA). HCOOH, H_2O_2 (30%) and H_2SO_4 (95%–97%) were provided from Merck (North America), and $C_4K_2O_9Ti{\cdot}2H_2O$ was obtained from Sigma-Aldrich (USA).

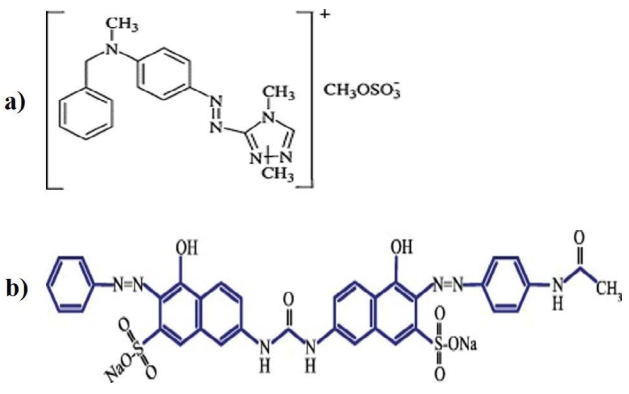

Fig. 1. Chemical structures of (a) BR 46 and (b) DR 23.

The stock solutions of 1,000 mg/L of BR 46 and DR 23 were first prepared and then the desired dye concentrations were prepared by appropriate dilutions from stock dye solutions. The pHs of the solutions were adjusted with 0.1 N hydrochloric acid and 0.1 N sodium hydroxide.

2.2. Green synthesis of Pd/Fe_3O_4 bimetallic nanoparticles

The lemon leaves were firstly washed with distilled water and then air-dried at ambient temperature. For the preparation of extract, 10 g of dried leaves were boiled in 500 mL of distilled water in a beaker under continuously stirring for 60 min. For the green synthesis of Pd/Fe_3O_4 NPs, 0.5 g of $FeSO_4{\cdot}7H_2O$ and 0.1 g of $PdCl_2$ were dissolved in 60 mL aqueous extract of the lemon leaves at 60°C under vigorous stirring. Then, a solution of 1.0 M Na_2CO_3 was added dropwise to the mixture to obtain alkaline pH while changing the color to dark brown. After being stirred again for 3 h at the same temperature, a suspension was formed which gave a precipitate of Pd/Fe_3O_4 NPs on centrifugation and the obtained nanoparticles were washed with distilled water, respectively, and then dried at 105°C in an oven [22].

2.3. Characterization of Pd/Fe_3O_4 NPs

The morphology of the Pd/Fe_3O_4 NPs was analyzed by scanning electron microscopy (SEM) Zeiss SUPRA 55 SEM analysis (Jena Germany). The mean hydrodynamic particle size and size distribution of the green synthesized Pd/Fe_3O_4 NPs were measured by dynamic light scattering (DLS) analysis with the Malvern Instruments Ltd., UK. The crystal structure was observed by X-ray diffraction (XRD) analysis using nickel-filtered Cu Kα radiation in a Philips (Eindhoven, Netherlands) X'PERT MPD apparatus operated at 40 kV and 30 mA, in the 2θ range of 10°–90°.

2.4. Heterogeneous Fenton-like decolorization experiments with in-situ generated H_2O_2

In-situ generation of hydrogen peroxide was performed by formic acid decomposition and O_2/air in the batch system. Heterogeneous Fenton-like decolorization experiments with in-situ H_2O_2 generation was conducted in Erlenmeyer flasks (250 mL) containing 100 mL of dye solutions in a shaker that was adjusted 25°C of temperature and constant shaking speed of 90 stroke/min.

In the experiments, 0.1 g of Pd/Fe_3O_4 NPs, except for catalyst concentration experiments, was added to solutions containing 5 mL of desired concentrations of formic acid and 100 mL of dye solutions at known initial dye concentrations, and they were agitated in the water bath at a constant temperature. The initial pH of dye solutions was adjusted by 0.1 N HCl or 0.1 N NaOH solutions. Air was passed into the reaction medium as an oxygen source with aquarium pumps for 2 h and then the air was turned off. Subsequently, dye concentrations were monitored by sampling at regular time intervals and analyzed by using the ultraviolet-visible (UV-vis) spectrophotometer.

Furthermore, heterogeneous Fenton-like decolorization experiment with in-situ generated H_2O_2 with the real textile wastewater including binary dye mixture of BR 46 and DR 23 was conducted at the environmental conditions of initial pH of 3.0, the formic acid concentration of 1,000 mM, and the catalyst concentration of 3.0 g/L.

2.5. Analytical methods

The decolorization percentages were expressed in terms of the decrease in UV-vis absorbances at the wavelength of 530 and 507 nm for BR 46 and DR 23, respectively, and calculated with Eq. (1) as given follow:

$$D(\%) = \frac{A_0|_{t=0} - A_t|_{t=t}}{A_0|_{t=0}} \times 100 \quad (1)$$

where D(%) represented the color removal efficiency, A_0 was the initial absorbance of dye solutions at t = 0 min, and A_t was the absorbance of dye solutions at t min.

In the experiments conducted with real textile wastewater, the decolorization efficiency was determined by the UV-vis absorbance measurement at the wavelength of 530 nm which was the maximum wavelength obtained by UV-vis spectral scan for real textile wastewater contaminated by BR 46 and DR 23 dyes mixture.

To verify the in-situ generated H_2O_2, the deionized water was used instead of dye solution and generated H_2O_2 was measured by a photometric method using potassium titanium oxide oxalate dihydrate as chromogenic reagent at 390 nm.

3. Results and discussions

3.1. Characterization of green synthesized Pd/Fe_3O_4 bimetallic nanoparticles

SEM images of green synthesized Pd/Fe_3O_4 NPs at different magnifications are presented in Figs. 2a–d. In the SEM images of Pd/Fe_3O_4 NPs, the spherical nanosized Fe_3O_4 NPs particles and the rod-like Pd particles were observed. It was observed that, a good combination of Fe_3O_4 NPs and Pd. Fig. 2c shows the SEM images of spherical Fe_3O_4 NPs at a magnification of 100 KX, and Fig. 2d belongs to rod-like Pd particles at a magnification of 100 KX. As seen in Fig. 2c, Fe_3O_4 NPs are nanosize with a diameter ≈60 nm which was determined by the Image J program but, they are prone to agglomeration.

SEM images after heterogeneous Fenton-like decolorization of BR 46 and DR 23 azo dyes are presented in Figs. 3a–d. Figs. 3a and b show the SEM images of Pd/Fe_3O_4 NPs after heterogeneous Fenton-like decolorization of BR 46. As seen from Figs. 3a and b, it was observed that the morphological structure not changed significantly and Pd particles pervaded on Fe_3O_4 NPs surface. Figs. 3c and d show the SEM images of Pd/Fe_3O_4 NPs after heterogeneous Fenton-like decolorization of DR 23. As seen from Figs. 3c and d, the rod-like structures of Pd particles were clustered and caused to form flower-like structures and agglomerated Fe_3O_4 NPs were obtained.

The particle size distribution of the green synthesized Pd/Fe_3O_4 NPs was determined by DLS analysis and the results are presented in Fig. 4. As depicted in Fig. 4, nanoparticles were homogeneously distributed and their mean hydrodynamic particle radius was found to be 64.95 nm with a polydispersity index value of 0.370.

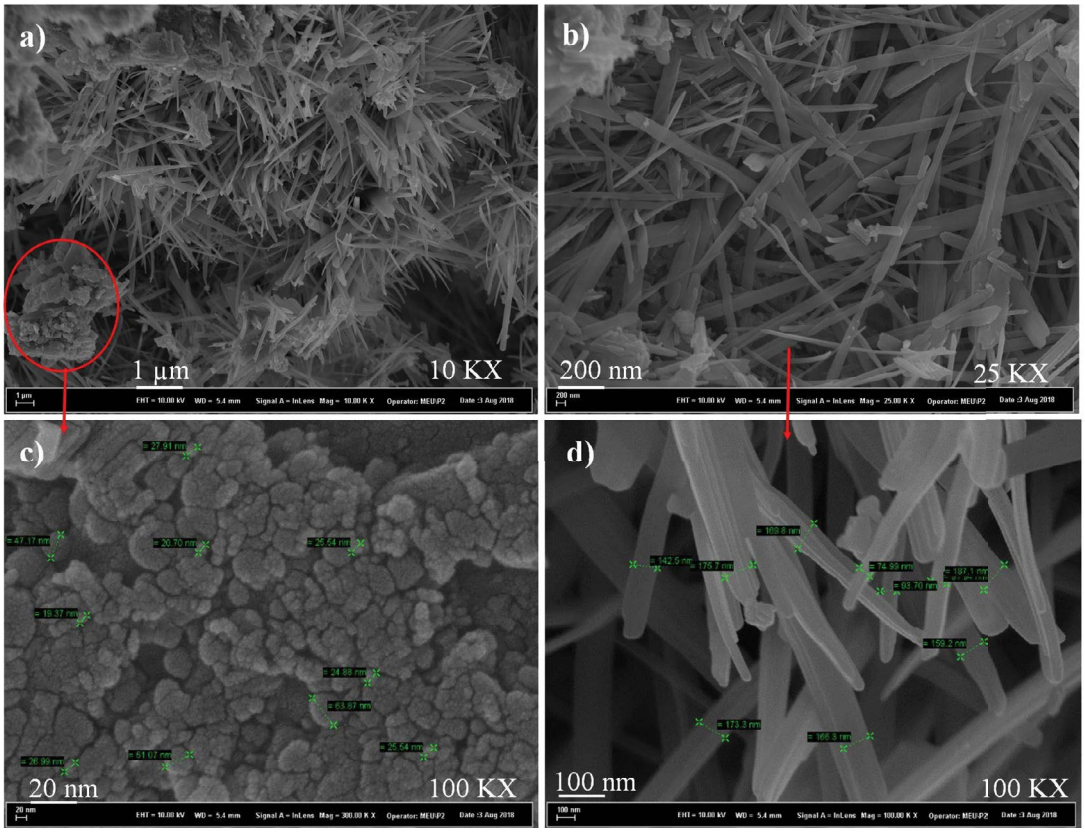

Fig. 2. SEM images of green synthesized Pd/Fe_3O_4 NPs at different magnifications.

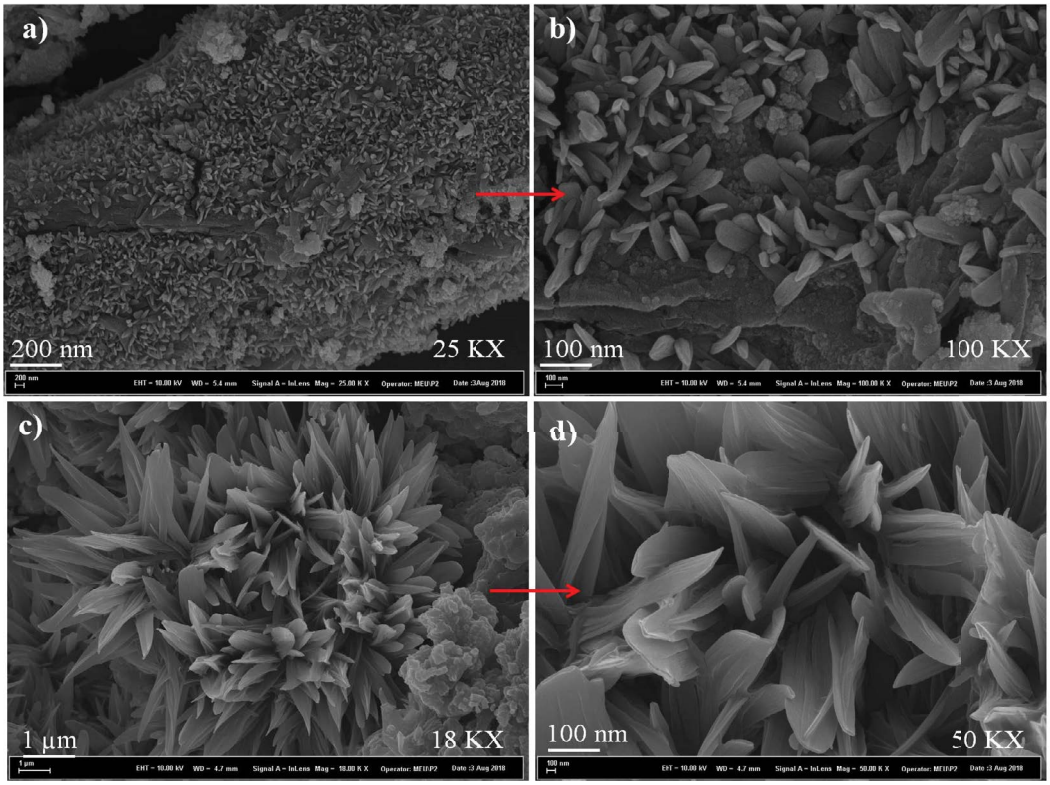

Fig. 3. SEM images of Pd/Fe_3O_4 NPs after heterogeneous Fenton-like decolorization of (a,b) BR 46 and (c,d) DR 23.

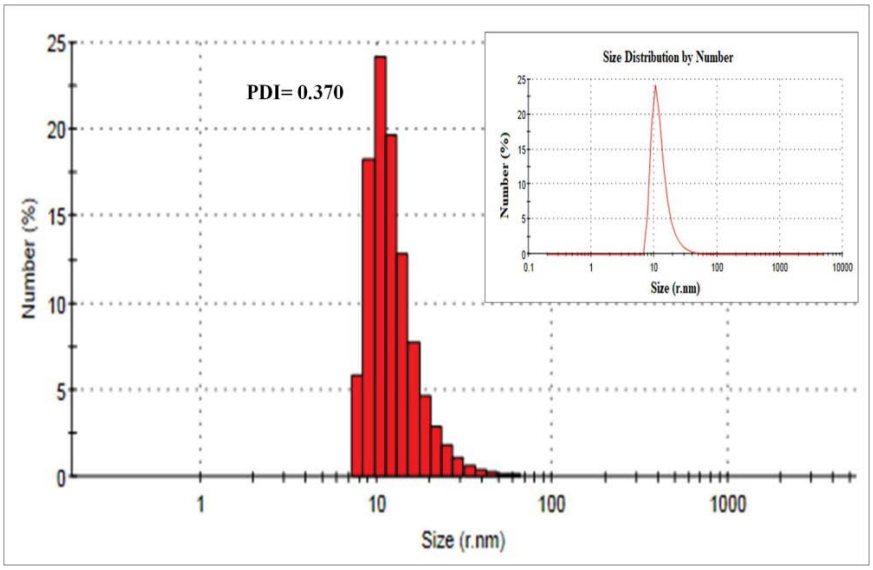

Fig. 4. The particle size distribution of Pd/Fe_3O_4 NPs.

The crystalline structure of synthesized bimetallic nanoparticles was confirmed with XRD measurements. The XRD pattern of the Pd/Fe_3O_4 is shown in Fig. 5. According to XRD analysis results, the presence of palladium and iron was confirmed in the structure of Pd/Fe_3O_4 NPs. The peaks at 40.08° and 46.69° corresponded to the (111) and (200) reflections of face-centered cubic Pd (JCPDS 46-1043). The peak at 35.60° was assigned to the (311) reflections of Fe_3O_4 [23]. Moreover, as can be seen from Fig. 5, the relatively weak peaks obtained in the XRD diagram indicated that the synthesized catalyst has amorphous parts. Moreover, some studies in the literature have reported that the synthesized nanoparticles by plant extracts are amorphous structure [24].

3.2. Influencing factors of heterogeneous Fenton-like decolorization of BR 46 and DR 23 with in-situ generated H_2O_2

3.2.1. Effect of initial pH

The pH value is one of the important parameters for the decolorization/degradation of organic pollutants, due to its effection in-situ generation of H_2O_2 from the decomposition of HCOOH by the catalyst and the generation of •OH from the decomposition of H_2O_2 by Fe(III) ions. Moreover, it is generally reported that a lower initial pH value provides the generation of •OH radicals and results in the higher removal efficiency of pollutants in the Fenton-like decolorization processes [25–27]. The initial pH effect on the heterogeneous

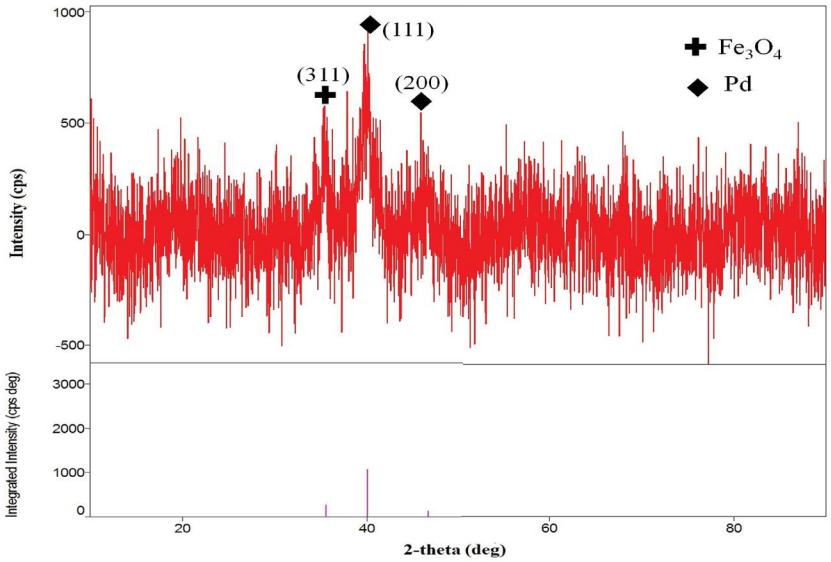

Fig. 5. XRD pattern of green synthesized Pd/Fe_3O_4 bimetallic nanoparticles.

Fenton-like decolorization of BR 46 and DR 23 with in-situ generated H_2O_2 is presented in Fig. 6. As seen in Fig. 6, the final removal efficiency of BR 46 was 97.56% at the reaction conditions of 10 h reaction time, 0.5 g/L of catalyst concentration, and initial pH of 3.0. The removal efficiencies of BR 46 decreased slightly when the pH of the solution was increased. On the other hand, according to Fig. 6, the final removal efficiency of DR 23 was 85.84% at the reaction conditions of 10 h reaction time, 1 g/L of catalyst concentration, and an initial pH of 3.0. The removal efficiency of DR 23; was 80.75%, 76.06%, and 74.23% at the initial pH values of 4.0, 5.0, and 6.0, respectively. As a result, initial pH 3.0 was proved to be more suitable for Fenton-like decolorization of BR 46 and DR 23 by the Pd/Fe_3O_4 NPs/O_2 process.

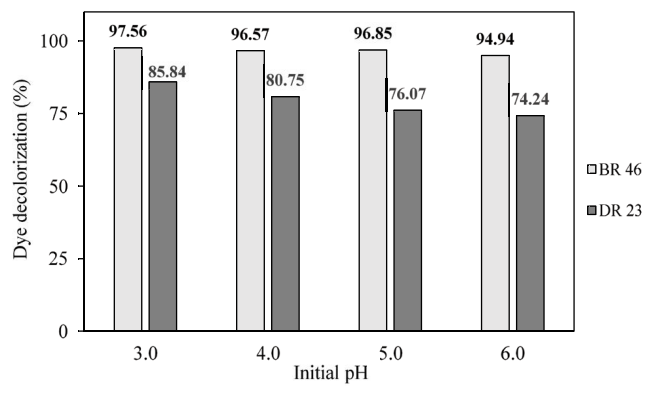

Fig. 6. Effect of initial pH (C_0 = 25 mg/L, C_{FA} = 500 mM, X_0 = 0.5 g/L (BR 46), X_0 = 1 g/L (DR 23), T = 25°C, time = 10 h).

3.2.2. Effect of catalyst concentration

The effect of catalyst concentration on the dye decolorizations in the Fenton-like process with in-situ generated H_2O_2 is presented in Fig. 7. As seen from Fig. 7, when the Pd/Fe_3O_4 NPs concentration was increased from 0.5 to 3 g/L, the BR 46 decolorization efficiency increased from 38.83% to 94.74%. This was mainly owing to the increasing amount of active sites to produce more reactive species such as H_2O_2 and •OH. So, 3 g/L of catalyst concentration was selected optimum to achieve the high BR 46 color removal efficiency. When the Pd/Fe_3O_4 NPs concentration was increased from 0.5 to 2 g/L, the DR 23 decolorization efficiency increased from 60.62% to 90.74%. However, the decolorization degree slightly decreased when the catalyst concentration was increased from 2.0 to 3.0 g/L, which was maybe attributed to the percentage of •OH scavenged by Fe(III) through undesirable reaction [28]. Thus, the optimum Pd/Fe_3O_4 NPs concentration was determined as 2 g/L for DR 23 decolorization.

3.2.3. Effect of formic acid concentration

In-situ generation of H_2O_2 was achieved through the reaction of formic acid and O_2. Formic acid was used as a source of hydrogen to produce H_2O_2 in this study. The in-situ H_2O_2 synthesis takes place with the reaction between formic acid and O_2 [9].

$$(HCOOH \rightarrow H_2(g) + CO_2(g) \quad (\Delta G_{298\,K} = -35.0 \text{ kJ / mol})$$

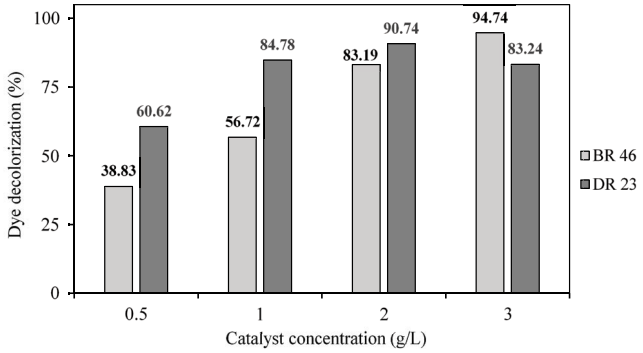

Fig. 7. Effect of catalyst concentration (C_0 = 25 mg/L, C_{FA} = 500 mM, pH = 3.0, T = 25°C, time = 10 h (DR 23), time = 2 h (BR 46)).

The researchers reported that formic acid can be decomposed over Pd to CO_2 and H_2 which further reacts with O_2 to produce H_2O_2 [17]. Therefore, the optimum formic acid concentration should be determined, due to, it is related to the number of hydroxyl radicals produced during the reaction. The effect of formic acid concentration for BR 46 and DR 23 decolorization is presented in Fig. 8. According to Fig. 8, the highest decolorization percentage was obtained in 1,000 mM of formic acid concentration for BR 46, and 500 mM of formic acid concentration was selected optimum for DR 23 decolorization. The reason of decreasing the decolorization percentage of DR 23 during in-situ generation of hydrogen peroxide at 1,000 mM of formic acid concentration may be due to the deactivating the catalyst by avoiding dye molecules to be exposed to the generated hydrogen peroxide or by consumption of generated H_2O_2 or •OH by formic acid itself. Therefore, 500 mM was found to be favorable for DR 23 decolorization.

3.2.4. Effect of the initial BR 46 and DR 23 concentrations

The effect of initial dye concentration on BR 46 and DR 23 decolorization is presented in Figs. 9a and b, respectively. The results showed that the removal efficiencies of BR 46 were 94.70%, 95.64%, 95.12%, and 95.71% when BR 46 concentrations were 25, 50, 100, and 200 mg/L, respectively after 5 h reaction time. Also, the removal efficiencies of DR 23 were 90.47%, 90.38%, and 85.18% when DR 23 concentrations were 25, 50, and 75 mg/L, respectively after 10 h. A bit lower removal efficiency was obtained for DR 23 at higher initial dye concentration, was due to more DR 23 dye was available in the solution for oxidation. Also, as seen from Figs. 9a and b, catalyst blank experiments (without catalyst, bubbling O_2 in HCOOH added dye solutions) were carried out. When O_2 passed into the reaction medium, no detectable activity towards dye decolorization was observed.

Additionally, the adsorbent property of Pd/Fe_3O_4 NPs was investigated in the same experimental conditions but the absence of formic acid and H_2O_2. These adsorption experiments showed that almost no color removal percentages were obtained in both two dyes. Therefore, it was believed that the decolorization mechanism of both dyes depends on the in-situ generation of H_2O_2 and also, Fe and

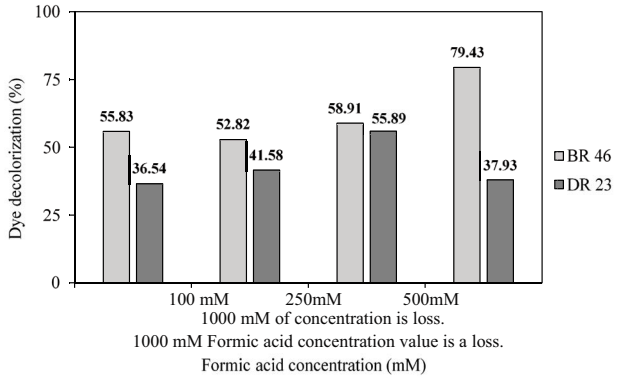

Fig. 8. Effect of formic acid concentration (C_0 = 25 mg/L, X_0 = 0.5 g/L, pH = 3.0, T = 25°C, time = 5 h).

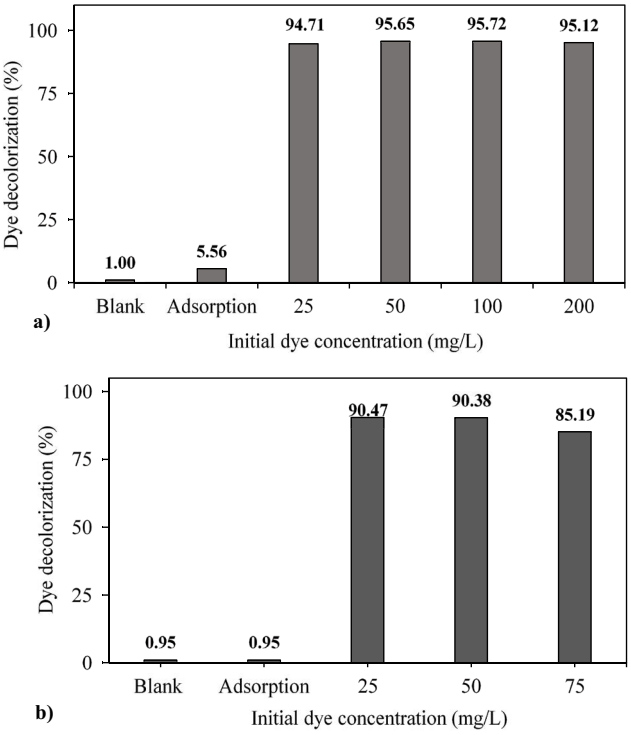

Fig. 9. Effect of initial dye concentration (a) BR 46 (C_{FA} = 1,000 mM, X_0 = 3 g/L, pH = 3.0, T = 25°C, time = 5 h, blank C_0 = 25 mg/L, adsorption C_0 = 25 mg/L) and (b) DR 23 (C_{FA} = 500 mM, X_0 = 2 g/L, pH = 3.0, T = 25°C, time = 10 h, blank C_0 = 25 mg/L, adsorption C_0 = 25 mg/L).

Pd played important roles in the synergistic effect, that is, Pd nanoparticles worked in in-situ H_2O_2 generations by formic acid decomposition and Fe nanoparticles worked in decompose H_2O_2 for generating •OH radicals for decolorization of BR 46 and DR 23.

Moreover, heterogeneous Fenton-like decolorization experiments of BR 46 and DR 23 with in-situ generated H_2O_2 were monitored by UV-vis spectral analysis. Changes in the absorption spectrum of dyes are given in Figs. 10a and b, respectively. Also, the progress of the decolorizations is given in the inset of Figs. 10a and b. According to

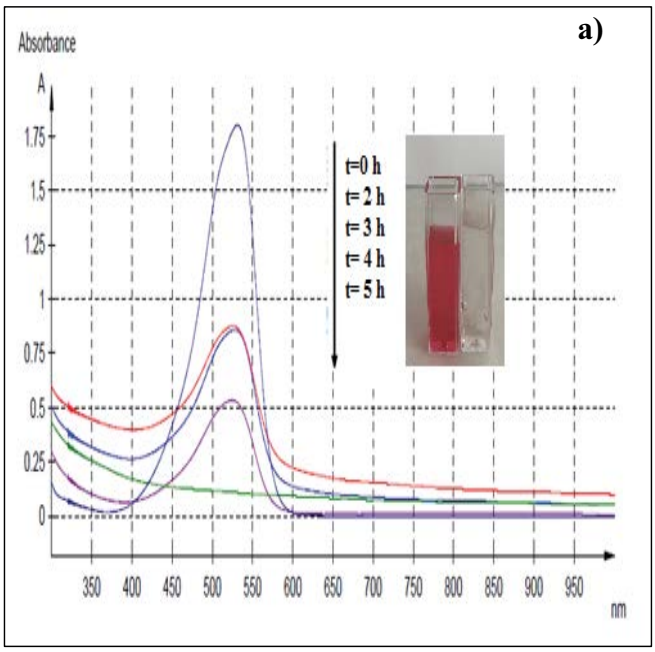

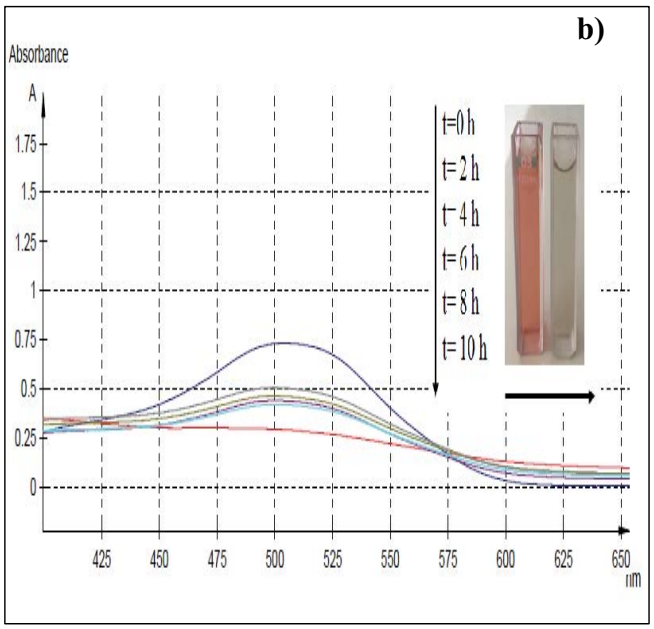

Fig. 10. UV-vis spectra of dye solutions after decolorization (a) BR 46 (C_0 = 25 mg/L, C_{FA} = 1,000 mM, X_0 = 3 g/L, pH = 3.0, T = 25°C, time = 5 h) and (b) DR 23 (C_0 = 25 mg/L, C_{FA} = 500 mM, X_0 = 2 g/L, pH = 3.0, T = 25°C, time = 10 h).

Figs. 10a and b, in the visible region, the broad bands at 530 and 507 nm result from the conjugated π system, linked by the two azo groups which are responsible for the color of BR 46 dye and DR 23 dye, respectively. Consequently, with the increase of the reaction time, the adsorption peaks gradually declined and approximately disappeared, which suggested that the chromophoric group (N=N group) in the dye molecular structures were broken as well as conjugated system and eventually the BR 46 and DR 23 molecules were decolorized.

3.2.5. Determination of in-situ generated H_2O_2

In order to confirm the in-situ generated H_2O_2, the deionized water instead of dye solution was used and the generated H_2O_2 was determined. The obtained results are presented in Fig. 11. As seen in Fig. 11, no significant H_2O_2 was formed in the catalyst blank experiment (without catalyst, bubbling air/O_2 in HCOOH added deionized water). The accumulation concentration of H_2O_2 in the system was 8.34 mg/L at 2 h reaction time, and 10.30 mg/L at 6 h reaction time, after that the concentration of H_2O_2 decreased slightly. As a result, the catalytic system included the simultaneous generation of hydrogen peroxide from formic acid and oxygen, the formation of hydroxyl radicals, and the oxidation of dyestuffs, so the catalytic system was effective despite low concentration of H_2O_2.

The examples of the studies in the literature about the Fenton-like degradation of various organic substances with in-situ H_2O_2 synthesis are presented in Table 1. As seen from Table 1, in this study, the high decolorization efficiencies were achieved at reasonable in-situ generated H_2O_2 concentration for BR 46 in the range of 25–200 mg/L of dye concentrations, and for DR 23 in the range of 25–75 mg/L dye concentrations. As a result, Pd/Fe_3O_4 NPs can provide effective treatment as a heterogeneous Fenton-like catalyst for the wastewaters containing anionic and cationic dyes, in a single step without adding H_2O_2 from outside to the reaction medium.

3.3. Decolorization of BR 46 and DR 23 in real textile wastewater

The real textile wastewater sample was provided by a textile company in Turkey. The properties of the real textile wastewater were presented in our previous study [30]. It is not known which dyestuffs are present in the real textile wastewater because the identification of its structure could not be provided by the supplier. Therefore, the binary mixture of BR 46 and DR 23 dyes (4 mL–25 mg/L of each dye) was added to the 20 mL of real textile wastewater to investigate the removal efficiency of this method. The experiment with the real textile wastewater was carried out at the obtained optimum environmental conditions of initial pH of 3.0, the formic acid concentration of 1,000 mM,

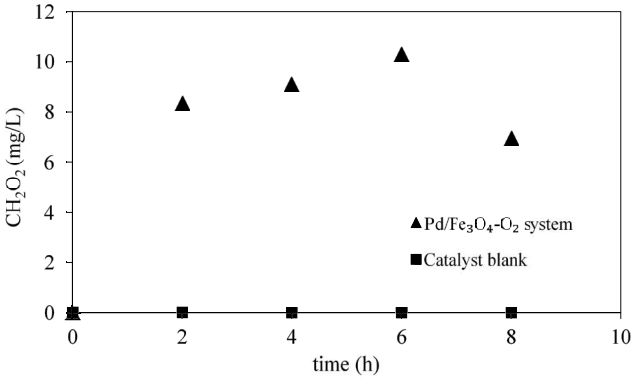

Fig. 11. Directly detect the in situ generated H_2O_2 by spectrophotometric determination (50 mL of deionized water, pH = 3, 2 g/L of catalyst, 500 mM of HCOOH).

Table 1
Some studies in the literature on the heterogeneous Fenton-like degradation of various organic substances with the in-situ synthesis of H_2O_2

Contaminant	Catalyst/oxidant	$C_{[Contaminant]}$	$C_{[Catalyst]}$	pH/T(°C)	*D* (%)	COD/TOC	Method	References
Phenol	Semi-heterogeneous Pd/Al_2O_3 + soluble Fe^{2+} catalyst/in-situ H_2O_2	100 mg/L	0.1 g	3–4/–3–4 and 7–9	–	TOC: %35	Fenton-like reaction (H_2 substituted organic component: formic acid, hydrazine, and hydroxylamine)	[16]
	FePd/Al_2O_3 heterogeneous catalyst/in-situ H_2O_2					TOC: %21		
Acid Red 73	SBA-15 supported Pd/PdO/Fe_2O_3 NPs/in-situ H_2O_2	100 mg/L	0.6 g/L	3/25°C	99	–	Fenton-like reaction (H_2 substituted organic component: formic acid)	[17]
Calmagite	Mn(II)/iron NH_2OH in-situ H_2O_2	0.1 mM	50 mM 1.50 mM 100 mM	8/20	90	–	H_2 substitue organic component	[29]
Basic Red 46	Pd/Fe_3O_4 NPs	25–200 mg/L	3 g/L	3/25	(94.71–95.12)	–	Fenton-like reaction (H_2 substituted organic component: formic acid)	This study
Direct Red 23	in-situ H_2O_2	25–75 mg/L	2 g/L		(90.47–85.19)			

D: Decolorization

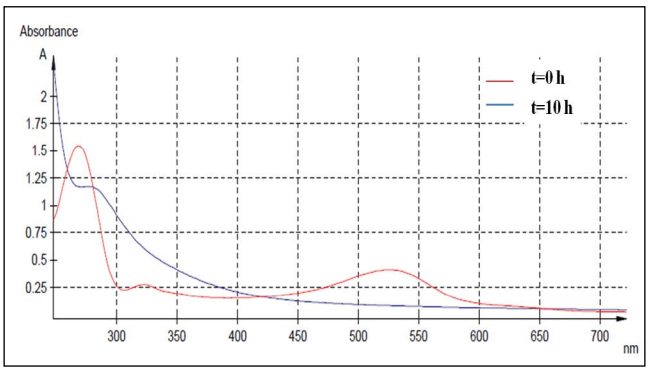

Fig. 12. UV-vis spectra of real textile wastewater including binary dye mixture of BR 46 and DR 23 (C_0 = 25 mg/L, C_{FA} = 1,000 mM, X_0 = 3 g/L, pH = 3.0, T = 25°C, time = 10 h).

temperature 25°C and the catalyst concentration of 3.0 g/L at 10 h reaction time.

The decolorization percentage for real textile wastewater including binary dye mixture of BR 46 and DR 23 was calculated in terms of the decrease in the intensity at the corresponding λ_{max} at 530 nm. The absorption spectra of BR 46 and DR 23 overlapped and so, only one maximum absorption band at 530 nm was obtained for the binary dye mixture of BR 46 and DR 23 in the real wastewater sample. Therefore, the total decolorization percentage was determined for real textile wastewater including binary dye mixture of BR 46 and DR 23. Changes in the UV-vis spectral analysis spectrum of real wastewater with time was presented in Fig. 12.

As seen in Fig. 12, the absorption band of binary dyestuff mixture at 530 nm which is responsible for the color of dyestuffs declined at the end of the 10 h reaction time. Moreover, the absorption band of the wastewater sample at 260 nm decreased a bit with time. Therefore, it can be concluded that the catalyst provided both the decolorization of a binary mixture of studied model dyes and also some degree of the other contaminants in the real textile wastewater.

According to obtained results, 80.56% decolorization efficiency was achieved for real wastewater including a binary mixture of dyes. These results showed that Pd/Fe_3O_4 NPs exhibited the effective catalyst property both in-situ H_2O_2 formation and Fenton-like decolorization. Hence, this treatment system could be used effectively in industrial wastewater treatment plants thanks to being efficient, cost-effective and simple.

4. Conclusions

In the present work, Pd/Fe_3O_4 nanoparticles were established as an efficient catalyst for in-situ generation of hydrogen peroxide and heterogeneous Fenton-like catalytic reaction. In the synthesis step of Pd/Fe_3O_4 NPs using a green, renewable reagent such as lemon (*Citrus limon (L.) Burm. f.*) leaves aqueous extract a great advantage in terms of environment, economy, and sustainability. According to characterization results, it was determined that the morphological structure of material composed of the good combination of the spherical nanosized Fe_3O_4 particles, and the rod-like Pd particles. The mean hydrodynamic particle radius of Pd/Fe_3O_4 NPs was measured to be 64.95 nm by DLS analysis. Moreover, the XRD diagram demonstrated that the crystal structure of synthesized nanoparticles was Pd/Fe_3O_4 because of the presence of characteristic peaks of iron and Pd.

The heterogeneous Fenton-like decolorization experiments with in situ generated H_2O_2 were carried out to investigate the effects of operational parameters on the decolorization of studied model dyes. The highest decolorization yields were achieved at the end of 5 h reaction time with an initial pH of 3.0, catalyst concentration of 3.0 g/L, and formic acid concentration of 1,000 mM for BR 46 in the range of 25–200 mg/L. The optimum conditions for 25 mg/L of initial DR 23 concentration were determined as the initial pH of 3.0, catalyst concentration of 2.0 g/L, and formic acid concentration of 500 mM. The obtained results showed that Pd/Fe_3O_4 NPs were more effective as a heterogeneous Fenton-like catalyst for anionic dye BR 46 than cationic dye DR 23 when considering the reaction time and initial dye concentration range. Moreover, 80.56% decolorization efficiency was obtained for real textile wastewater including a binary mixture of studied dyes.

In the BR 46 and DR 23 dye decolorization with in-situ generated H_2O_2, the catalytic system involves the simultaneous generation of H_2O_2 from HCOOH by Pd centers of catalyst, and the decomposition of H_2O_2 into hydroxyl radicals by Fe centers. The good collaboration of the active species made the reaction system work well in spite of the low concentration of H_2O_2 was detected in the reaction media. Therefore, this system could be utilized effectively for the degradation of many toxic organic contaminants in wastewaters with no need for the extra addition of H_2O_2 to reaction media. Thus, developing the single catalyst for both pollutant removal by the Fenton-like process and in-situ synthesis of H_2O_2 which is the provider of $^{\bullet}OH$ radicals for degradation process is quite satisfactory with regard to the process economy. The worldwide production of H_2O_2 exceeds 2,200,000 t/a with an annual growth rate prediction of 4%, so the production cost is enormous. Moreover, there are many important challenges in the synthesis of H_2O_2 like that the synthesis methods are expensive and require the use of hazardous chemicals and the use of H_2/O_2 mixtures which shows the explosive property. Therefore, improving the production and use efficiency of H_2O_2 is very important for touch on the global energy, environmental and economic aspects. The obtained results from this study showed that the approach of in-situ production of H_2O_2 could be beneficial in terms of process cost thanks to avoiding the invalid consumption of H_2O_2 in the degradation of contaminants. Also, the green synthesis of a catalyst from the plant leaves contributes to the process economy because they are environmentally friendly, abundant, inexpensive.

Consequently, the synthesized green catalyst displayed excellent performances for anionic and cationic dye removal by heterogeneous Fenton-like catalytic reaction with the in-situ generation of hydrogen peroxide. The insights from this study can help in smarter catalyst design to get rid of some challenges that prevent the widespread utilizing of Fenton-like catalysts and efficient treatment of organic contaminants from industrial wastewaters.

Acknowledgments

This work was supported by BAP, Scientific Research Projects Management of Mersin University, Turkey, (Project code: 2018-3-TP3-3047).

References

[1] N. Wang, T. Zheng, G.S Zhang, P. Wang, A review on Fenton-like processes for organic wastewater treatment, J. Environ. Chem. Eng., 4 (2016) 762–787.
[2] S.Y. Park, J.W. Lee, J.H. Song, T.J. Kim, Y.-M. Chung, S.H. Oh, I.K. Song, Direct synthesis of hydrogen peroxide from hydrogen and oxygen over Pd/HZSM-5 catalysts: effect of Brönsted acidity, J. Mol. Catal. A: Chem., 363 (2012) 230–236.
[3] N. Tan, Z. Yang, X.-B. Gong, Z.-R. Wang, T. Fu, Y. Liu, In situ generation of H_2O_2 using MWCNT-Al/O_2 system and possible application for glyphosate degradation, Sci. Total Environ., 650 (2019) 2567–2576.
[4] P. Landon, P.J. Collier, A.F. Carley, D. Chadwick, A.J. Papworth, A. Burrows, G.J. Hutchings, Direct synthesis of hydrogen peroxide from H_2 and O_2 using Pd and Au catalysts, Phys. Chem. Chem. Phys., 5 (2003) 1917–1923.
[5] J.K. Edwards, N. Ntainjua, A.F. Carley, A.A. Herzing, C.J. Kiely, G.J. Hutchings, Direct synthesis of H_2O_2 from H_2 and O_2 over gold, palladium, and gold–palladium catalysts supported on acid-pretreated TiO_2, *Angew. Chem. Int. Ed.*, 48 (2009) 8512–8515.
[6] B.E. Solsona, J.K. Edwards, P. Landon, A.F. Carley, A. Herzing, C.J. Kiely, G.J. Hutchings, Direct synthesis of hydrogen peroxide from H_2 and O_2 using Al_2O_3 supported Au–Pd catalysts, Chem. Mater., 18 (2006) 2689–2695.
[7] Y.J. Huang, X.C. Zhou, M. Yin, C.P. Liu, W. Xing, Novel PdAu@Au/C core–shell catalyst: Superior activity and selectivity in formic acid decomposition for hydrogen generation, Chem. Mater., 22 (2010) 5122–5128.
[8] S. Zhang, Y.Y. Shao, H.-G. Liao, J. Liu, I.A. Aksay, G.P. Yin, Y.H. Lin, Graphene decorated with PtAu alloy nanoparticles: facile synthesis and promising application for formic acid oxidation, Chem. Mater., 23 (2011) 1079–1081.
[9] Z.-L. Wang, Y. Ping, J.-M. Yan, H.-L. Wang, Q. Jiang, Hydrogen generation from formic acid decomposition at room temperature using a NiAuPd alloy nanocatalyst, Int. J. Hydrogen Energy, 39 (2014) 4850–4856.
[10] Z.Y. Zhang, S.-W. Cao, Y. Liao, C. Xue, Selective photocatalytic decomposition of formic acid over AuPd nanoparticle-decorated TiO_2 nanofibers toward high-yield hydrogen production, Appl. *Catal., B*, 162 (2015) 204–209.
[11] S.-J. Li, Y. Ping, J.-M. Yan, H.-L. Wang, M. Wu, Q. Jiang, Facile synthesis of AgAuPd/graphene with high performance for hydrogen generation from formic acid, J. Mater. Chem. A., 3 (2015) 14535–14538.
[12] K. Tedsree, T. Li, S. Jones, C.W.A. Chan, K.M.K. Yu, P.A. Bagot, E.A. Marquis, G.D.W. Smith, S.C.E. Tsang, Hydrogen production from formic acid decomposition at room temperature using a Ag–Pd core–shell nanocatalyst, Nat. Nanotechnol., 6 (2011) 302.
[13] K. Mori, S. Masuda, H. Tanaka, K. Yoshizawa, M. Che, H. Yamashita, Phenylamine-functionalized mesoporous silica supported PdAg nanoparticles: a dual heterogeneous catalyst for formic acid/CO_2-mediated chemical hydrogen delivery/storage, Chem. Commun., 53 (2017) 4677–4680.
[14] M.S. Yalfani, S. Contreras, F. Medina, J. Sueiras, Direct generation of hydrogen peroxide from formic acid and O_2 using heterogeneous Pd/γ-Al_2O_3 catalysts, Chem. Commun., (2008) 3885–3887, doi: 10.1039/b803149e.
[15] V.R. Choudhary, P. Jana, *In situ* generation of hydrogen peroxide from reaction of O_2 with hydroxylamine from hydroxylammonium salt in neutral aqueous or non-aqueous medium using reusable Pd/Al_2O_3 catalyst, Catal. Commun., 8 (2007) 1578–1582.
[16] M.S. Yalfani, S. Contreras, F. Medina, J.E. Sueiras, Hydrogen substitutes for the *in situ* generation of H_2O_2: an application in the Fenton reaction, J. Hazard. Mater., 192 (2011) 340–346.
[17] X.F. Li, X. Liu, L. Xu, Y.Z. Wen, J.Q. Ma, Z.C. Wu, Highly dispersed Pd/PdO/Fe_2O_3 nanoparticles in SBA-15 for Fenton-like processes: confinement and synergistic effects, Appl. Catal., B, 165 (2015) 79–86.
[18] N.A.N. Mohamad, N.A. Arham, J. Jai, A. Hadi, Plant extract as reducing agent in synthesis of metallic nanoparticles: a review, Adv. Mater. Res., 832 (2014) 350–355.
[19] D.J. Mabberley, Citrus (Rutaceae): a review of recent advances in etymology, systematics and medical applications, Evol. Biogeogr. Plants, 49 (2004) 481–498.
[20] W. Konicki, I. Pełech, E. Mijowska, I. Jasińska, Adsorption of anionic dye Direct Red 23 onto magnetic multi-walled carbon nanotubes-Fe_3C nanocomposite: kinetics, equilibrium and thermodynamics, Chem. Eng. J., 210 (2012) 87–95.
[21] F. Deniz, S. Karaman, Removal of Basic Red 46 dye from aqueous solution by pine tree leaves, Chem. Eng. J., 170 (2011) 67–74.
[22] M. Nasrollahzadeh, S.M. Sajadi, A. Rostami-Vartooni, M. Khalaj, Green synthesis of Pd/Fe_3O_4 nanoparticles using *Euphorbia condylocarpa M. bieb* root extract and their catalytic applications as magnetically recoverable and stable recyclable catalysts for the phosphine-free Sonogashira and Suzuki coupling reactions, J. Mol. Catal. A: Chem, 396 (2015) 31–39.
[23] H.A. Elazab, A.R. Siamaki, S. Moussa, B.F. Gupton, M.S. El-Shall, Highly efficient and magnetically recyclable graphene-supported Pd/Fe_3O_4 nanoparticle catalysts for Suzuki and Heck cross-coupling reactions, Appl. Catal., A, 491 (2015) 58–69.
[24] T. Shahwan, S.A. Sirriah, M. Nairat, E. Boyacı, A.E. Eroğlu, T.B. Scott, K.R. Hallam, Green synthesis of iron nanoparticles and their application as a Fenton-like catalyst for the degradation of aqueous cationic and anionic dyes, Chem. Eng. J., 172 (2011) 258–266.
[25] Y. Kuang, Q.P. Wang, Z.L. Chen, M. Megharaj, R. Naidu, Heterogeneous Fenton-like oxidation of monochlorobenzene using green synthesis of iron nanoparticles, J. Colloid Interface Sci., 410 (2013) 67–73.
[26] J.-H. Sun, S.-P. Sun, G.-L. Wang, L.-P. Qiao, Degradation of azo dye Amido black 10B in aqueous solution by Fenton oxidation process, Dyes Pigm., 74 (2007) 647–652.
[27] M. Neamtu, A. Yediler, I. Siminiceanu, A. Kettrup, Oxidation of commercial reactive azo dye aqueous solutions by the photo-Fenton and Fenton-like processes, J. Photochem. Photobiol., A, 161 (2003) 87–93.
[28] Y. Liu, Q. Fan, J.L. Wang, Zn-Fe-CNTs catalytic in situ generation of H_2O_2 for Fenton-like degradation of sulfamethoxazole, J. Hazard. Mater., 342 (2018) 166–176.
[29] T.S. Sheriff, S. Cope, M. Ekwegh, Calmagite dyeoxidation using *in situ* generated hydrogen peroxide catalysed by manganese(II) ions, Dalton Trans., 44 (2007) 5119–5122.
[30] M. Ergüt, D. Uzunoğlu, A. Özer, Efficient decolourization of malachite green with biosynthesized iron oxide nanoparticles loaded carbonated hydroxyapatite as a reusable heterogeneous Fenton-like catalyst, J. Environ. Sci. Health. Part A Toxic/Hazard. Subst. Environ. Eng., 54 (2019) 1–15.